Journal of Luminescence 153 (2014) 96–103

Contents lists available at ScienceDirect

Journal of Luminescence

journal homepage: www.elsevier.com/locate/jlumin

On the shape of continuous wave infrared stimulated luminescence signals from feldspars: A case study

V. Pagonis [a,*], M. Jain [b], K.J. Thomsen [b], A.S. Murray [c]

[a] McDaniel College, Physics Department, Westminster, MD 21157, USA
[b] Center for Nuclear Technologies, Technical University of Denmark, DTU Risø Campus, DK-4000 Roskilde, Denmark
[c] Nordic Laboratory for Luminescence Dating, Department of Earth Sciences, Aarhus University, Risø DTU, DK-4000 Roskilde, Denmark

ARTICLE INFO

Article history:
Received 19 December 2013
Received in revised form
24 February 2014
Accepted 3 March 2014
Available online 13 March 2014

Keywords:
Feldspar
IRSL curves
Random defect model

ABSTRACT

The continuous-wave IRSL (CW-IRSL) signals from feldspars are known to decay in a non-exponential manner, and their exact mathematical description is of great importance in dosimetric and dating studies. This paper investigates the possibility of fitting experimental CW-IRSL curves from a variety of feldspar samples, by using an analytical equation derived within the framework of a new model based on localized electronic recombinations of donor–acceptor pairs. 24 different types of feldspars were studied and their CW-IRSL signals are analyzed in order to establish the range and precision of numerical values for the fitting parameters in the analytical equation. The study finds systematic trends in the fitting parameters, and possible systematic differences between K and Na rich extracts from the same feldspar samples. Furthermore, results are compared with natural samples, freshly irradiated samples, and samples which had undergone anomalous fading. The results of this analysis establish broad numerical ranges for the fitting parameters in the model. Specifically the possible range of the dimensionless density ρ' was found to be $\rho' \sim 0.002–0.01$. These experimentally established ranges of ρ' will help to guide future modeling work on luminescence processes in feldspars. Small statistical differences were found between K-rich and Na-rich fractions of the same sample. However, the experimental data shows that the parameters depend on the irradiation dose, but do not depend on the time elapsed after the end of the irradiation process. All samples exhibited the power law of decay, with the range of the power law coefficient $\beta = 0.6–1.1$.

1. Introduction

Over the past 20 years there has been considerable experimental and modeling work trying to understand the nature and properties of luminescence signals from feldspars, especially in connection with the associated phenomenon of "anomalous fading" based on quantum mechanical tunneling (see for example [1–3]). The continuous-wave IRSL signals (CW-IRSL, also known as "infrared shine down" curves) from these materials are known to decay in a non-exponential manner and their origin as well as their exact mathematical description is an open research question. Mathematical and physical characterization of the shape of these CW-IRSL signals in feldspars is of great importance in dosimetric and dating studies (Refs. [4–32]).

There is an abundance of experimental data as well as significant modeling work in the literature which suggests that the dominant process in anomalous fading in feldspars is tunneling from the ground state or via the excited state, or from both. Poolton et al. [7–8,17] explained IRSL in feldspars using a donor–acceptor model, in which electron tunneling occurs from the excited state and the band tail states of the IRSL trap at about 1.4 eV. Thomsen et al. [22,23] suggested that in this model, the beginning of the IRSL decay curve originates with the luminescence emitted from close donor–acceptor pairs, while the end of the IRSL curve most likely represents the tunneling of distant pairs. The recent experimental work by Poolton et al., [17], Jain and Ankjærgaard [18], Ankjærgaard et al. [19], Andersen et al. [31] and Kars et al. [32] provided valuable information on the origin of these CW-IRSL signals and support the presence of several competing mechanisms during the luminescence process. These mechanisms involve the tunneling processes in localized recombinations taking place from the ground and excited state of the trap, as well as charge migration through the conduction band-tail states.

There have also been significant developments in the modeling aspects of the luminescence mechanism for CW-IRSL signals, including the experimentally observed empirical power law of decay in feldspars ([14–16]). Kars et al. [11] and Larsen et al. [12] presented new types of models involving localized tunneling transitions, while Pagonis et al.

* Corresponding author. Tel.: +1 410 857 2481; fax: +1 410 386 4624.
E-mail address: vpagonis@mcdaniel.edu (V. Pagonis).

http://dx.doi.org/10.1016/j.jlumin.2014.03.010
0022-2313/

[20] presented a new empirical kinetic model, in an attempt to describe tunneling via the excited state in feldspars. In an important development in this research area, Jain et al. [21] presented a new general kinetic model which quantifies localized electronic recombination of donor–acceptor pairs in luminescent materials. Recombination is assumed to take place via the excited state of the donor, and to take place between nearest-neighbors within a random distribution of centers. Two versions of the model were presented: an exact model that evolves in both space and time, and an approximate semi-analytical model that evolves only in time. These authors found good agreement between the two models, and simulated successfully both thermally stimulated luminescence (TL) and optically stimulated luminescence (OSL). The model also demonstrated the power law behavior for OSL signals simulated within the model.

Pagonis et al. [33] examined the full model by Jain et al. [21], and obtained analytical expressions for the distribution of remaining donors at any time t during the following experimental situations: TL, OSL, linearly modulated OSL and infrared stimulated luminescence (LM-OSL, LM-IRSL) and isothermal TL (ITL). These authors gave examples for the derived distributions of donors in each experimental case, and similarities and differences between the different experimental modes of stimulation were pointed out. They also demonstrate how LM-IRSL signals in feldspars can be analyzed using the model, and what physical information can be extracted from such experimental data. Their analytical equations were tested by fitting successfully a series of experimental LM-IRSL data for Na- and K-feldspar samples available in the literature.

Kitis and Pagonis [34] showed that the system of simultaneous differential equations developed by Jain et al. [21] can be approximated to a very good precision by a single differential equation describing stimulated luminescence emission in this system. These authors were able to obtain analytical solutions of this single differential equation for several possible modes of stimulation, namely TL, OSL, LM-OSL and ITL. They also derived the exact analytical form for the power law behavior in this system, and demonstrated how typical experimental TL glow curves and CW-IRSL signals can be analyzed using the derived analytical equations, and what physical information can be extracted from such experimental data.

The goals of the present paper are as follows.

(a) To investigate the possibility of fitting experimental CW-IRSL curves from a variety of feldspar samples by using the analytical equation derived by Kitis and Pagonis [34] within the framework of the model by Jain et al. [21].
(b) To investigate the range of numerical values, as well as the precision of the kinetic parameters derived from fitting experimental data to the analytical equation derived by Kitis and Pagonis [34]. Special attention is paid in looking for systematic trends in the fitting parameters, and for possible systematic differences between K and Na rich extracts from the same feldspar samples.
(c) To compare the fitting parameters obtained from CW-IRSL curves measured in 3 types of samples: natural samples, freshly irradiated samples, and samples which have undergone anomalous fading. The specific goal here is to search for possible effects of laboratory irradiation and anomalous fading on the shape of the CW-IRSL signals.
(d) To examine the power law decay of these signals from different types of feldspars.

2. Analytical solution for CW-IRSL signals within the model of Jain et al. [21]

In this section we summarize briefly the main physical assumptions and equations used in the model of Jain et al. [21], and discuss the analytical equation used in this paper to fit experimental CW-IRSL curves. The main physical assumption in the model of Jain et al. [21] is the presence of a random distribution of hole traps in the luminescent volume, and an associated range of random nearest-neighbor recombination probabilities. Within the model, stimulated recombination takes place only via the excited state of the electron trap, by either optical or thermal stimulation. The concentration of holes is assumed to be much larger than the population of electrons in traps so that there is no redistribution of electron–hole distances during the experiment, and an electron can tunnel only to its nearest hole. In the exact form of the model, one writes a system of differential equations describing the traffic of electrons between the ground state, the excited state and the recombination center. These coupled differential equations contain two variables, namely the distance r' between donor–acceptor pairs and the time t.

Jain et al. [21] also developed an approximate semi-analytical model to describe the behavior of the system. This second version of the model evolves only in time, and the approximation used is based on introducing a critical tunneling lifetime τ_c. The equations in the approximate semi-analytical model version of the model and for the case of CW-IRSL experiments are [21]as follows:

$$\frac{dn_g}{dt} = -An_g + Bn_e, \tag{1}$$

$$\frac{dn_e}{dt} = An_g - Bn_e - \frac{3n_e\rho'^{1/3}}{\tau_c}\left(\ln\frac{n_o}{n}\right)^{2/3} z, \tag{2}$$

$$L(t) = -\frac{dm}{dt} = \frac{3n_e\rho'^{1/3}}{\tau_c}\left(\ln\frac{n_o}{n}\right)^{2/3} z, \tag{3}$$

$$\tau_c = s^{-1}\exp\left[\left(\frac{1}{\rho'}\ln\frac{n_o}{n}\right)^{1/3}\right]. \tag{4}$$

The following parameters and symbols are used in these expressions: n_g and n_e are the instantaneous concentrations of electrons in the ground state and in the excited state correspondingly. m is the instantaneous concentration of acceptors (holes), n is the instantaneous concentration of all the donors, and N represents the instantaneous concentration of electrons in thermally disconnected states, such that $m = n + N = (n_g + n_e) + N$. The parameter A represents the excitation rate from the ground to the excited state, and is equal to $A = \sigma(\lambda)I$ for the case of optical excitation. Here λ is the optical stimulation wavelength, $\sigma(\lambda)$ is the optical absorption cross-section and I is the light intensity ($\mathrm{cm^{-2}\,s^{-1}}$). Additional parameters are the dimensionless number density of acceptors ρ', the critical tunneling lifetime τ_c, the thermal excitation frequency factor s, and $z = 1.8$ – a dimensionless constant introduced in the model.

B ($\mathrm{s^{-1}}$) is the relaxation rate from the excited into the ground state, and $L(t)$ is the instantaneous tunneling luminescence from recombination via the excited state. Under the detailed balance principle one also has $B = s$. Perhaps the most important physical parameter in the model is the dimensionless number density of acceptors ρ' and the critical tunneling lifetime τ_c which depends on the instantaneous concentration of donors n as shown in Eq. (4). Jain et al. [21] simulated successfully both TL and optically stimulated luminescence (OSL) processes in their model, and also demonstrated the power law behavior for simulated OSL signals within the model. However, their approximate semi-analytical model was found to disagree with the exact solution of the model in the case of low values of the optical excitation probabilities $A = 1$–$10\ \mathrm{s^{-1}}$ (Ref. [21, Fig. 7a and 7b]).

Kitis and Pagonis [34] showed that under certain simplifying physical assumptions, the system of Eqs. (1)–(4) can be replaced

accurately with a single differential equation, and they obtained the following analytical solution for the CW-IRSL luminescence intensity $L(t)$ at time t:

$$L(t) = 3n_o\rho' F(t)^2 zAe^{-F(t)}e^{-\rho'[F(t)]^3} \quad (5)$$

with the quantity $F(t)$ defined by

$$F(t) = \ln\left(1+z\int_0^t Adt'\right) = \ln(1+zAt). \quad (6)$$

By substituting Eq. (6) into (5), the following analytical equation is obtained:

$$L(t) = \frac{C[\ln(1+zAt)]^2 e^{-\rho'[\ln(1+zAt)]^3}}{1+zAt} \quad (7)$$

where C is a constant amplitude which depends on the experimental conditions. Eq. (7) is used to fit the experimental CW-IRSL curves in this paper. The three variable fitting parameters are C, ρ', A It is noted that for $t=0$ Eq. (7) gives $L=0$. Furthermore, for $t<1$ s the intensity $L(t)$ of the CW-IRSL signal will increase, while for $t>1$ s it will decrease monotonically. In practical terms this means that the first 1 s of the experimental CW-IRSL data should not be included in the fitting procedure.

3. Analysis of IRSL curves from a suite of $N=24$ feldspar samples

A first experimental study was carried out to investigate the possibility of fitting CW-IRSL curves from a variety of feldspar samples by using the analytical Eq. (7).

It is to be noted that Eq. (7) was developed for a full distribution of nearest neighbor distances. In a natural or a laboratory irradiated sample that has undergone preheating, it is expected to have a truncated distribution since the pairs with a small lifetime will have recombined because of thermal excitations. Nonetheless for a preliminary investigation it is convenient to directly use Eq. (7) for fitting, rather than doing multiple simulations first for preheat and then for CW-IRSL. At the moment it is not clear what the overall error induced by such a simplification is; it may change somewhat the absolute value of the model parameters obtained by the fitting procedure. However, since all investigations presented here are done in a relative mode (comparison across different doses, or delay times, or different samples), it is quite likely that this issue is not significant for the present preliminary investigation.

The suite of museum feldspar samples listed in Table 1 is chosen to represent a wide variety of samples, and also because it contains pairs of Na- and K-rich fractions extracted from the same feldspar samples (referred to as NF and KF in the rest of this paper and in some of the figures). The main goal of this experiment is to establish the range and precision of the numerical values for the fitting parameters C, ρ', A. A second goal is to search for any systematic differences in the fitting parameters from natural and laboratory irradiated samples, as well as searching for possible differences between the available pairs of K- and Na- rich fractions.

The experimental sequence is as follows: a natural sample is preheated for 60 s at 320 °C, followed by measurement of the CW-IRSL signal by optical stimulation at 50 °C for 500 s at 90% of full optical power. Immediately afterwards the sample undergoes CW-IRSL stimulation for 100 s at an elevated temperature of 325 °C, in order to empty the dosimetric trap. Subsequently the same aliquot is irradiated for 300 s and the complete sequence is repeated to measure the CW-IRSL signal for the irradiated aliquot. The complete experimental sequence is then repeated for the rest of the $N=24$ samples/aliquots shown in Table 1.

Table 1
List of feldspar samples analyzed in this paper. KF and NF indicate K-rich and Na-rich fractions of the same sample.

Sample position in disk	Sample no.	Sample lab code	Feldspar type/name
1	1	981007	FK
3	2	981007	NF
5	3	075403	FK
7	4	075403	NF
9	5	092203	FK
11	6	092203	NF
13	7	K-Feldspar	Spain
15	8	Microcline	
17	9	970203	KF
19	10	970203	NF
21	11	Labrador icing	90–180 μm
23	12	102205	FK
25	13	102203	FK
27	14	H22550	FK
29	15	095201	FK
31	16	Oligoclase	90–180 μm
33	17	Albite sweden	70–180 μm
35	18	A4-Anni	180–250 μm
37	19	095201	FN
39	20	065414	FK 180–250 μm
41	21	093071	FK 90–180 mm
43	22	072255	
45	23	AHO16	
47	24	082105	

Fig. 1a shows the result of fitting a typical CW-IRSL curve from K-rich (solid symbols) and Na-rich (open symbols) fractions of sample 981007. Only the first 100 s of the fitted signal are shown for clarity. The inset of Fig. 1a shows the complete experimental data extending to 500 s, on a log–log scale. The data points were measured 0.5 s apart, for a total of 1000 data points collected along the CW-IRSL curve. The best fitting values of the three parameters in Eq. (7) are $C=6.8\times10^5$ cnts/0.5 s, $\rho'=0.0063$ and $A=4.30$ s^{-1} for the K-rich fraction, and $C=8.9\times10^5$ cnts/0.5 s, $\rho'=0.0052$ and $A=4.10$ s^{-1} for the Na-rich fraction of the feldspar sample. The residuals of the fitting procedure representing the difference between the experimental data and the corresponding best fit values are shown below the fitted graph for the K-rich sample, and are seen to be better than ~5% of the corresponding CW-IRSL intensity for all points along the CW-IRSL signal. Typical R^2 values for these fits are $R^2=0.998$ indicating very good fits to the data. Fig. 1b shows the distribution of the residuals fitted to a Gaussian function centered at zero; despite a somewhat less satisfactory fit to the beginning of the data, an overall good global fit indicates that the residuals can be considered as a reasonable approximation to white noise. At least part of this systematic deviation at the beginning of the curve may arise from working with truncated nearest distributions rather than full distributions as assumed in the derivation of Eq. (7).

Figs. 2 and 3 show the fitting results obtained for CW-IRSL curves (obtained similarly as the ones shown in Fig. 1) from the 24 samples given in Table 1. Fig. 2a shows the results for the dimensionless density ρ', for both natural samples (filled circles) and for laboratory irradiated samples (open circles). The average values of ρ' were $\rho'=0.0037\pm0.0017$ (1σ) for natural and $\rho'=0.0050\pm0.0012$ $(1\sigma)$for the laboratory irradiated samples correspondingly. These results indicate that the (1σ) precision of the extracted fitting parametersρ' is of the order of ~24% for laboratory irradiated samples and ~46% for natural samples. The error bars shown on the left hand side of Fig. 2a indicate the size of the standard deviation of the data, and the horizontal dashed and solid lines indicate the positions of the average values. Fig. 2b shows the same data as in Fig. 2a in the form of histogram distributions. Inspection of the average values and standard deviations of the data in Fig. 2a

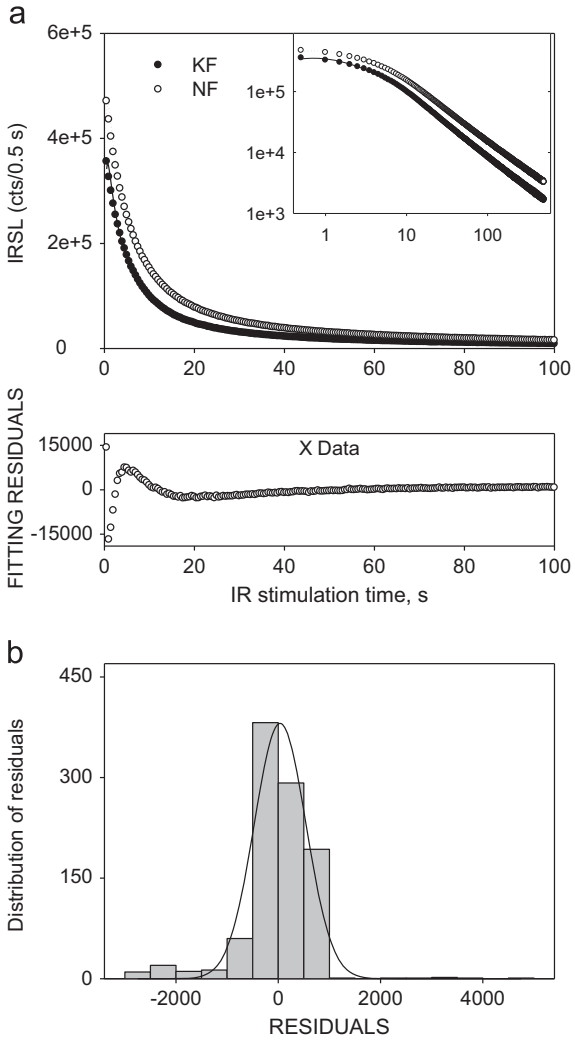

Fig. 1. (a) The result of fitting a typical CW-IRSL curve for K-rich and Na-rich fractions of the same feldspar sample (solid and open circles correspondingly) using Eq. (7). Only the first 100 s of the fitted signal are shown for clarity. The inset shows the complete experimental data extending to 500 s, on a log–log scale. The residuals of the fitting procedure are shown below the fitted graph of the K-rich sample. (b) The distribution of the residuals fitted to a Gaussian function centered at zero, indicating that the residuals can be considered as a reasonable approximation to white noise.

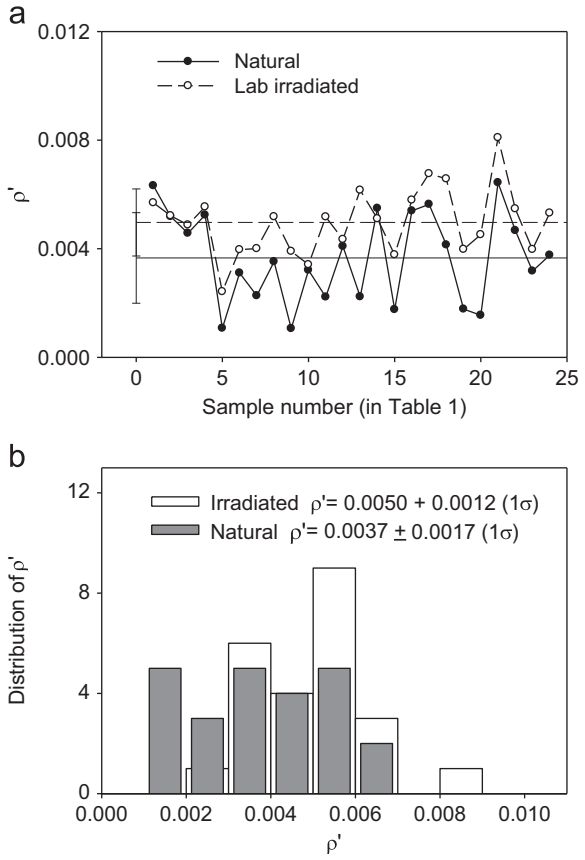

Fig. 2. The results of analyzing $N=24$ experimental CW-IRSL curves from the 24 feldspar samples in Table 1 using Eq. (7) by Kitis and Pagonis [34]. (a) The dimensionless densityρ', for both samples irradiated in nature (filled circles) and for laboratory irradiated samples (open circles). The error bars shown on the left hand side of the figure indicate the size of the standard deviation of the data, and the horizontal dashed and solid lines indicate the positions of the average values. (b) The same data as in (a) but shown in the form of histogram distributions.

and b shows that even though some systematic differences may exist between the ρ'values of the natural and irradiated samples, the difference between the two sample populations is not statistically significant.

Fig. 3a shows the best fitting values for the optical excitation probability of the 24 samples, with average values of $A=5.8\pm 2.3$ (s^{-1}) (1σ) and $A=6.1\pm 2.2$ (s^{-1}) $(1\sigma)$for the natural and irradiated samples, respectively. These results indicate that the precision of the extracted fitting parameter A isof the order of $\sim$36% for laboratory irradiated samples and $\sim$40% for natural samples. Clearly the data indicates that there is no significant statistical difference between the A values for natural and irradiated samples.

Fig. 3b shows the best fitting values for the constant C in Eq. (7); this constant is proportional to the intensity of the CW-IRSL curve at time $t=0$. As may be expected, there is wide variation in the values of C, which covers approximately 4 orders of magnitude from C$\sim$100 to C$\sim 10^6$ (cts/0.5 s). This data indicates again that there are no apparent systematic differences between the C values for natural and irradiated samples.

4. Analysis of prompt and faded CW-IRSL curves

Thomsen et al. [22] determined fading rates for sedimentary feldspar samples using both different stimulation and detection windows. They investigated the fading rates for both the initial part and the final part of the luminescence signal, and found that stimulation at elevated temperatures reduces the apparent fading rates. These authors concluded that some luminescence signals from sedimentary feldspars fade at a much lower rate than conventional IRSL signals. In the same work these authors determined the g-values by carrying out a series of sensitivity corrected measurements (L_x/T_x measurements) using a modified SAR procedure [28,29]. During these measurements, sensitivity changes are explicitly corrected by the use of a test dose (T_x). Furthermore, a prompt measurement was undertaken after each delayed measurement, in order to correct any further sensitivity changes occurring over time. Optical stimulation was carried out at 50 °C for 100 s, and a standard preheat of 60 s at 250 °C followed each irradiation [29]. The delay times between the end of irradiation and measurement of the CW-IRSL signals varied from a few seconds for prompt measurements, to long delays up to $\sim$17 h.

This section presents the results of fitting a series of L_x, T_x measurements carried out by Thomsen et al. [22]. However the current study is not concerned with the fading rates of the IRSL signal. Instead, the current analysis looks for systematic changes in the overall shape of the IRSL curve, by examining the behavior of the fitting parameters ρ' and A. The specific goal of the analysis is to show that one can fit accurately the L_x and T_x CW-IRSL curves

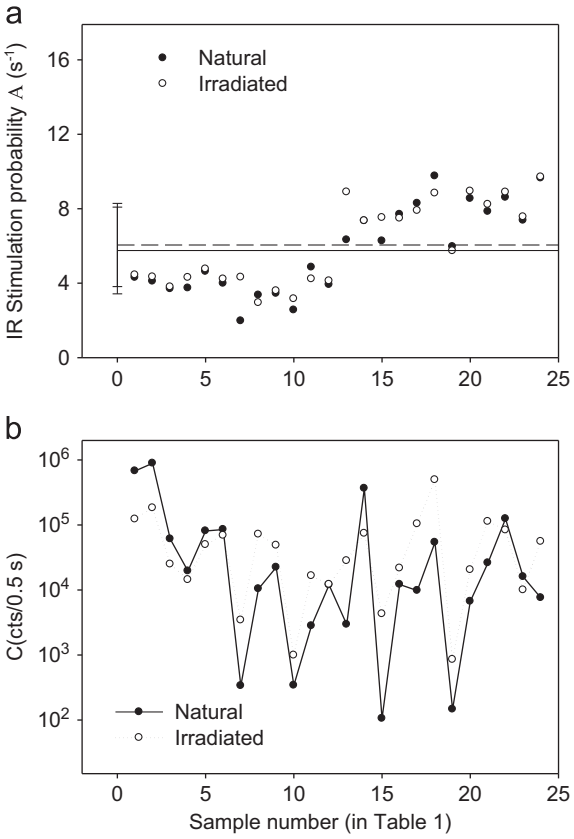

Fig. 3. (a) The best fitting values for the optical excitation probability of the $N=24$ samples for the naturally irradiated and the laboratory irradiated samples. This data does not support significant statistical differences between the A values for natural and irradiated samples. (b) The best fitting values for the constant C in Eq. (7); there is wide variation in the values of C covering approximately 4 orders of magnitude from $C\sim 100$ to $C\sim 10^6$ (cts/0.5 s).

using Eq. (7) from Kitis and Pagonis [34], and to investigate whether these signals can be characterized in a consistent manner. A secondary goal is to search for systematic differences in the fitting parameters from available pairs of K- and Na-rich fractions from the same feldspar samples.

Four feldspar samples were studied in detail. The first sample was a glaciofluvial feldspar from Russia (Laboratory number 963806, grain size 106–212 μm). The second sample was glaciofluvial feldspar from Greenland (Laboratory code 951020, 212–300 μm). Experimental CW-IRSL curves were analyzed from both K-rich and Na-rich extracts from each of these two samples, for a total of 4 samples studied.

The series of data that have been analyzed for each of these 4 samples consist of 12 L_x curves measured for each of 6 different aliquots of the same sample. This procedure yields a total of $N=12\times 6=72$ IRSL curves for the K-rich extracts, and an equal number of $N=72$ IRSL curves for the Na-rich extracts. An additional $N=72$ T_x curves were analyzed in each of these cases.

The $N=72$ curves analyzed for each sample represent a mixture of freshly irradiated states (prompt measurements), and states which have undergone anomalous fading for various elapsed times after irradiation (up to ~17 h). The specific goal here is to search for possible effects of laboratory irradiation and anomalous fading on the shape of the CW-IRSL signals. The results also provide an estimate of the reproducibility of the fitting parameters between different aliquots of the same sample, which can be considered as an estimate of the precision of this type of fitting curve analysis.

A typical result of the best fitting parameters obtained fitting $N=72$ L_x curves using Eq. (7) is shown in Fig. 4a (open circles). Also shown in the same Fig. 4a are $N=72$ data points obtained from analyzing the corresponding T_x curves (open triangles). It is noted that these T_x curves did not suffer any delay between irradiation and measurement of the CW-IRSL signals; they are plotted here on the same axis for illustration purposes. The sample analyzed in Fig. 4 is the K-rich extract of sample number 963806. The aliquots were irradiated for 600 s before measuring the L_x curves, and for 300 s with a dose rate of 0.045 Gy/s before measurement of the T_x curves. The error bars shown on the right hand side of Fig. 4a indicate the size of the standard deviation of the data (1σ), and the horizontal dashed and solid lines indicate the positions of the average values for the L_x and T_x curves.

Inspection of the data in Fig. 4a shows that there is no systematic correlation of the values of ρ' with the time delay after the end of irradiation. This seems to indicate that the shape of the CW-IRSL curves does not change very significantly during the modified SAR procedure used by Thomsen et al. [22]. However, the values of ρ' for the signals measured after 300 s of irradiation (~13.5 Gy, i.e. from the prompt T_x signals, triangles in Fig. 4a) are systematically lower than the corresponding ρ'values for the signals measured after 600 s of irradiation (~27 Gy for the L_x signals, circles in Fig. 4a). The average values of ρ' are $\rho' = 0.0063 \pm 0.0003$ (1σ) for the L_x signals, and $\rho' = 0.0057 \pm 0.0003$ (1σ) for the T_x signals. The histogram distribution of the same data is shown in Fig. 4b and it indicates

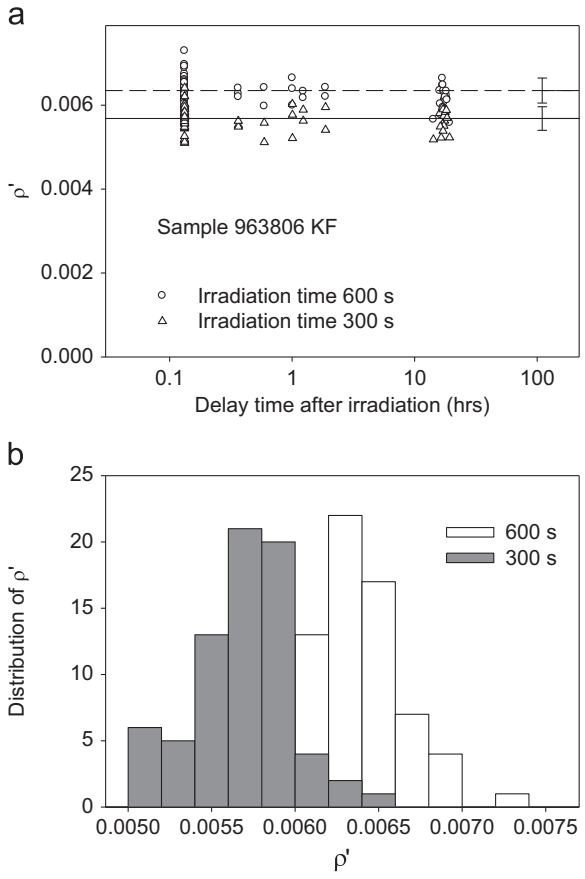

Fig. 4. Results of the best fitting ρ' parameters obtained fitting $N=72$ L_x curves from Thomsen et al. [22] using Eq. (7) (open circles). The open triangles are $N=72$ data points obtained from analyzing the corresponding T_x curves (open triangles). (a) The sample analyzed was the K-rich extract of sample number 963806. The error bars shown on the right hand side of this figure indicate the size of the standard deviation of the data(1σ), and the horizontal dashed and solid lines indicate the average values. (b) The same data as in (a) shown as a histogram distribution. The value of ρ' may depend on the irradiation dose.

that the value of ρ' may depend on the irradiation dose, although the size of the error bars in Fig. 4a shows two closely overlapping populations. The dependence of ρ'on the irradiation dose is an important experimental effect, which could have implications for both experimental work and for modeling. The presence of this effect was verified for the other samples in this study, although the effect seems to be stronger for some samples and weaker for others. It is noted that a recent experimental study by Morthekai et al. [35] also found evidence for a dependence of ρ'on the irradiation dose.

Fig. 5a shows the corresponding results for the optical excitation probability Aextracted from the T_x signals (open triangles) and the L_x signals (open circles). The values of A from the T_x signal are slightly lower than the corresponding values from the L_x signals, although the percentage difference between them is small (less than ~5%). The corresponding histogram distribution of the same data is shown in Fig. 5b, and the average values were $A=6.6\pm0.2$ (s^{-1}) for the L_x signals, and $A=6.8\pm0.2$ (s^{-1}) for the T_x signals. No systematic differences for the A values and no correlation of A with the delay time were apparent, at least within the precision of the experiments described here.

Fig. 6a shows a comparison of the ρ' values for the K-rich and Na-rich extracts of sample 963806. The data shown is for the L_x curves (samples irradiated for 600 s). Once more there is no apparent correlation of the values of ρ' with the delay time after the end of irradiation. Fig. 6b shows a similar comparison for the corresponding values of the optical excitation probability A for the K-rich and Na-rich samples. The data in Fig. 6a and b seem to

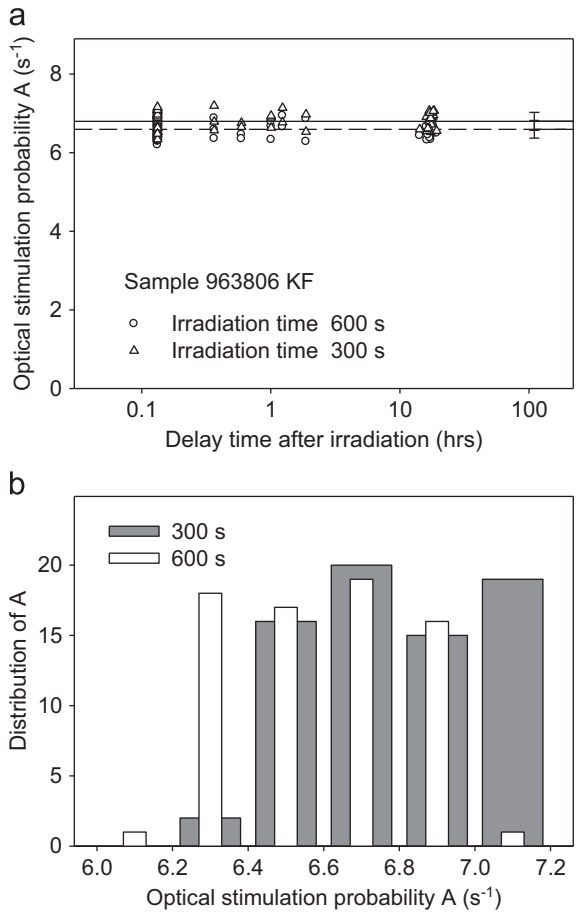

Fig. 5. (a) The results for the optical excitation probability A for the same sample 963806, with the T_x signals shown as open triangles and the L_x signals shown as open circles. (b) The corresponding histogram distribution of the same data as in (a). No systematic differences for the A values and no correlation of A with the delay time are apparent.

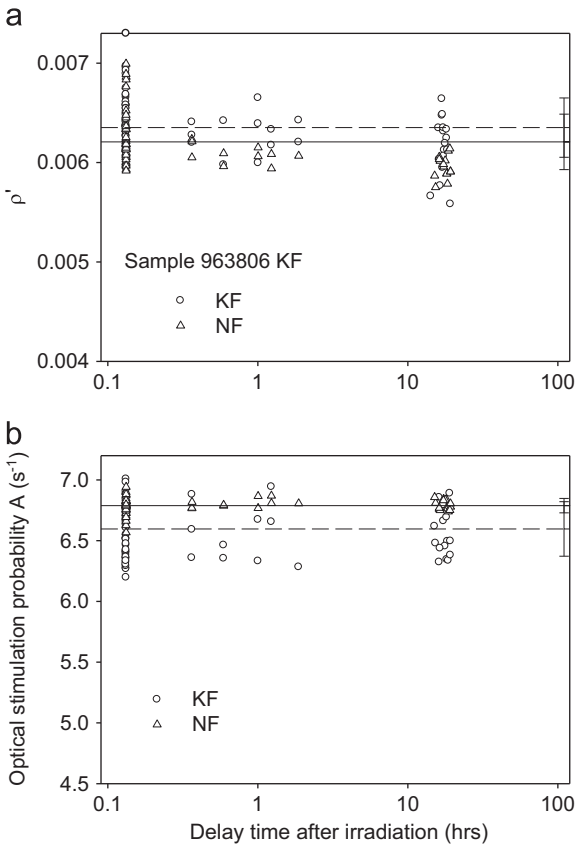

Fig. 6. (a) Comparison of the ρ'values for the K-rich and Na-rich extracts of sample 963806. The data shown is for the L_x curves (samples irradiated for 600 s). (b) A similar comparison for the corresponding values of the optical excitation probability A for the K-rich and Na-rich fractions of the same sample.

indicate no significant statistical differences between the two fractions of sample 963806, at least within the precision of the experiment.

Fig. 7 shows the same type of comparison for sample 951020. Fig. 7a shows the dimensionless charge density parameter ρ' for the Na-rich fraction (951020 NF) for two given doses of 400 s (~57 Gy, L_x curves) and 200 s (~28 Gy, T_x curves) as a function of delay time in the fading experiment. Once more the error bars in these figures indicate the size of the standard deviation of the data(1σ), and the horizontal dashed and solid lines indicate the average values of ρ' for the L_x and T_x curves. The data in Fig. 7b provides additional evidence that the value of ρ' may depend on the irradiation dose. The average values of ρ' are $\rho'=0.0056\pm0.0002$ (1σ) for the L_x signals, and $\rho'=0.0049\pm0.0002$ (1σ) for the T_x signals. Again no systematic correlation of the values of ρ' with the time delay is found. Fig. 7c shows the ρ' values obtained for the L_x curves (~57 Gy) for the K-rich and Na-rich fractions of sample 951020. Here we observe a statistically significant difference in ρ' between the two fractions. This difference was not observed for sample 963806 (see Fig. 6a).

Clearly further systematic experimental work is necessary in order to verify the effect of irradiation dose on the fitting parameters and on the shape of the CW-IRSL curves. In addition, more experimental work on different types of feldspars is necessary to ascertain (or not) any significant differences between K- and Na-rich fractions.

All the CW-IRSL curves analyzed in this paper displayed the power law behavior at long stimulation times. For example, the data in the inset of Fig. 1a show a linear behavior on a log–log scale

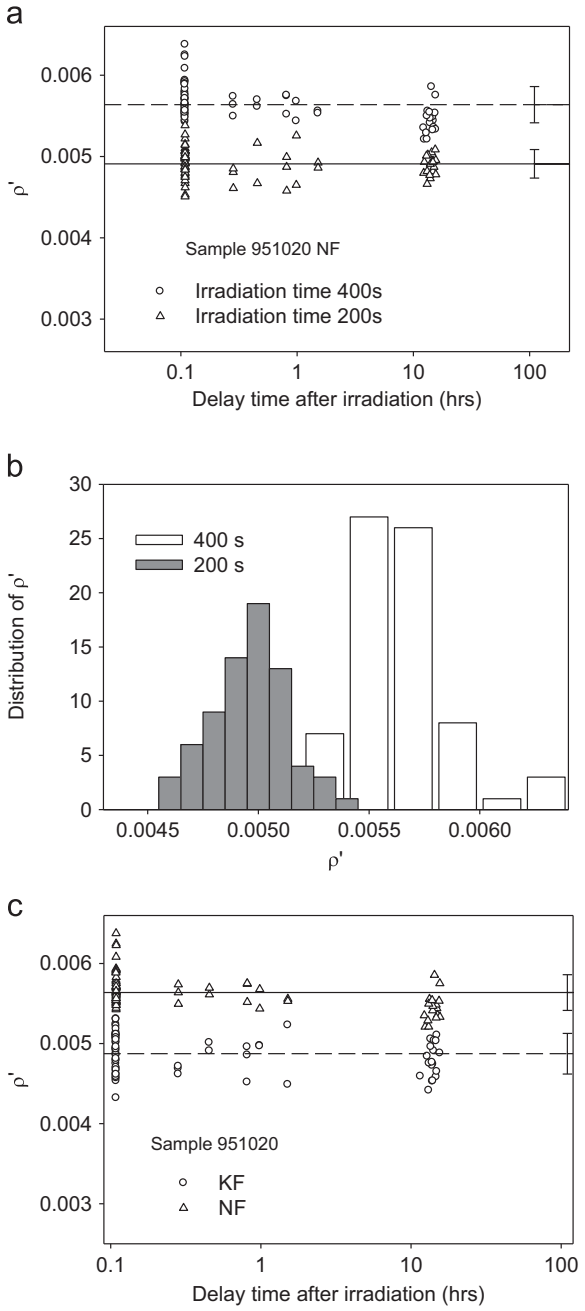

Fig. 7. (a) The results for the dimensionless charge density parameter ρ' for sample 951020. The aliquots were irradiated for 400 s before measuring the L_x curves, and for 200 s before measurement of the T_x curves. (b) The histogram distribution of the same data as in (a). (c) A comparison of the ρ'values for the K-rich and Na-rich extracts of sample 951020. The data shown is for the L_x curves (samples irradiated for 400 s). Some significant statistical difference between the two extracts is found within the precision of the experiment.

at long stimulation times, according to the power law behavior

$$\ln L(t) = c - \beta \ln t \tag{8}$$

where $L(t)$ is the luminescence intensity, t is the IR-simulation time and β is the dimensionless power law coefficient.

Fig. 8 shows an example of the distribution of the coefficient β for the K-rich fraction of sample 963806 and for both the L_x and T_x curves (600 s and 300 s irradiation times, respectively). The average values are $\beta = 0.84 \pm 0.10$ (1σ) for the L_x signals, and $\beta = 0.69 \pm 0.08$ (1σ) for the T_x signals. Once again, the histogram distribution of the data indicates that the value of β depends on

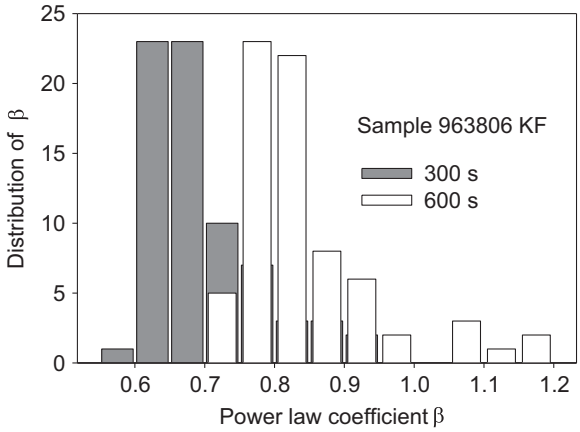

Fig. 8. The distribution of the coefficient β for the K-rich fraction of sample 963806 and for both L_x curves and T_x curves (600 s and 300 s irradiation times, respectively).

the irradiation dose, although the two populations closely overlap. The values of $\beta$are in agreement with previous experimental work by Bailiff and Poolton [24], Baril [16] and Bailiff and Barnett [27] who showed that the IRSL decay follows a power law type of decay. More generally, in some of these experimental studies the complete CW-IRSL signal was found to follow a Becquerel decay law of the form $A/(1+t/t_0)^{\beta}$ where A, β and t_0 are constants [36]. A comparison between Eq. (7) and Becquerel decay law will be presented elsewhere.

5. Discussion and conclusions

The results of this paper show that Eq. (7) can be used to fit accurately CW-IRSL signals from a variety of feldspar samples. The results establish broad numerical ranges for the fitting parameters C, ρ', Ain the model by Jain et al. [21] as applied to feldspars. Most notably, the range of the dimensionless density $\rho'$was found to be rather limited, from a low of $\sim$0.002 to a maximum of $\sim$0.01. These experimentally established ranges of ρ'will help to guide future modeling work on luminescence processes in feldspars.

The results also showed that the values of the fitting parameters may be statistically different for K-rich and Na-rich fractions of the same feldspar sample, however a more systematic study of this effect is necessary to establish the validity of these differences. The experimental data presented here seems to support some systematic dependence of the fitting parameters on the irradiation dose; the systematic increase in ρ' for higher dose for all samples suggests an increase in the concentrations of occupied holes and occupied trapping centers with dose. This systematic increase in ρ'can also be interpreted as due to a change in the *distribution of the distance between trapping and recombination centers.* The same effect has recently been documented by Morthekai et al. [35] using fading experiments after radiations of different ionization qualities. This phenomenon can have important consequences for future experimental and modeling work, especially with regard to fading correction. As expected, the time elapsed after the irradiation appears to have no significant statistical effect on the parameters$\rho'$and A. All samples examined here exhibit the power law of decay, with the range of values of the power law coefficient$\beta = 0.6$–1.1, in agreement with previous experimental studies.

Kitis and Pagonis [34] showed that the analytical Eq. (7) also applies to isothermal signals described by the model of Jain et al. [21]. In the case of isothermal experiments and for signals derived from a single trap, it is not clear at this point whether the

value of ρ'would be the same as the value derived from analysis of the CW-IRSL experiments. This is worth future investigations. A comparison of ρ' values for optical and thermal stimulation, as well as those estimated using laboratory fading experiments at room temperature will shed further light on the pathways used in these different recombination processes.

However, one would definitely expect the value of the stimulation probability A to strongly depend on the temperature used during the isothermal experiment. It is suggested that such a combined CW-IRSL and isothermal experiment on the same samples would provide valuable information on the luminescence processes in feldspars.

References

[1] L. Bøtter-Jensen, S.W.S. McKeever, A.G. Wintle, Optically Stimulated Luminescence Dosimetry, Elsevier, Amsterdam, 2003.
[2] R. Chen, S.W.S. McKeever, Theory of Thermoluminescence and Related Phenomena, World Scientific, Singapore, 1997.
[3] R. Chen, V. Pagonis, Thermally and Optically Stimulated Luminescence: A Simulation Approach, John Wiley & Sons, Chichester, 2011.
[4] R. Visocekas, Nucl. Tracks Radiat. Meas. 10 (1985) 521.
[5] R. Visocekas, N.A. Spooner, A. Zink, P. Blank, Radiat. Meas. 23 (1994) 371.
[6] G.A.T. Duller, L. Bøtter-Jensen, Radiat. Prot. Dosim. 47 (1993) 683.
[7] N.R.J. Poolton, J. Wallinga, A.S. Murray, E. Bulur, L. Bøtter-Jensen, Phys. Chem. Miner 29 (2002) 210.
[8] N.R.J. Poolton, K.B. Ozanyan, J. Wallinga, A.S. Murray, L. Bøtter-Jensen, Phys. Chem. Miner 29 (2002) 217.
[9] B. Li, S.-H. Li, Radiat. Meas. 46 (2010) 29.
[10] B. Li, S.H. Li, J. Phys. D 41 (2008) 225502.
[11] R.H. Kars, J. Wallinga, K.M. Cohen, Radiat. Meas. 43 (2008) 786.
[12] A. Larsen, S. Greilich, M. Jain, A.S. Murray, Radiat. Meas. 44 (2009) 467.
[13] D.J. Huntley, M. Lamothe, Can. J. Earth Sci. 38 (2001) 1093.
[14] C.J. Delbecq, Y. Toyozawa, P.H. Yuster, Phys. Rev. B 9 (1974) 4497.
[15] D.J. Huntley, J. Phys.: Condens. Matter 18 (2006) 1359.
[16] M.R. Baril, (Ph.D. thesis), Simon Fraser University, Burnaby, BC, Canada. Available online at: ⟨www.cfht.hawaii.edu/~baril/Temp/baril_phdthesis.pdf⟩, 2002.
[17] N.R.J. Poolton, R.H. Kars, J. Wallinga, A.J.J. Bos, J. Phys.: Condens. Matter 21 (2009) 485505.
[18] M. Jain, C. Ankjærgaard, Radiat. Meas. 46 (2011) 292.
[19] C. Ankjærgaard, M. Jain, R. Kalchgruber, T. Lapp, D. Klein, S.W.S. McKeever, A.S. Murray, P. Morthekai, Radiat. Meas. 44 (2009) 576.
[20] V. Pagonis, M. Jain, A.S. Murray, C. Ankjærgaard, R. Chen, Radiat. Meas. 47 (2012) 870.
[21] M. Jain, B. Guralnik, M.T. Andersen, J. Phys.: Condens. Matter 24 (2012) 385402 (12 pp.).
[22] K.J. Thomsen, A.S. Murray, M. Jain, L. Bøtter-Jensen, Radiat. Meas. 43 (2008) 1474.
[23] K.J. Thomsen, A.S. Murray, M. Jain, Geochronometria 38 (2011) 1.
[24] I.K. Bailiff, N.R.J. Poolton, Nucl. Tracks Radiat. Meas 18 (1991) 111.
[25] A.S. Murray, J.P. Buylaert, K.J. Thomsen, M. Jain., Radiat Meas. 44 (2009) 554.
[26] M.R. Baril, D.J. Huntley., J. Phys: Condens. Matter 15 (2003) 8011.
[27] I.K. Bailiff, S.M. Barnett, Radiat. Meas. 23 (1994) 541.
[28] A.S. Murray, A.G. Wintle., Radiat. Meas. 32 (2000) 57.
[29] M. Auclair, M. Lamothe, S. Huot, Radiat. Meas. 37 (2003) 487.
[30] A. Molodkov, I. Jaek, V. Vasilchenko, Geochronometria 26 (2007) 11.
[31] M.T. Andersen, M. Jain, P. Tidemand-Lichtenberg, J. Appl. Phys. 112 (2012) 043507.
[32] R.H. Kars, N.R.J. Poolton, M. Jain, C. Ankjærgaard, P. Dorenbos, J. Wallinga., Radiat. Meas. 59 (2013) 103.
[33] V. Pagonis, H. Phan, D. Ruth, G. Kitis., Radiat. Meas. 58 (2013) 66.
[34] G. Kitis, V. Pagonis., J. Lumin. 137 (2013) 109.
[35] P. Morthekai, M. Jain, G. Gach, D.R. Elema, H. Prip, J. Lumin. 143 (2013) 704.
[36] M.N. Berberan-Santos, E.N. Bodunov, B. Valeur, Chem. Phys. 317 (2005) 57.